

REPORT DOCUMENTATION PAGE				Form Approved OMB No. 0704-0188	
<p>Public reporting burden for this collection of information is estimated to average 1 hour per response, including the time for reviewing instructions, searching existing data sources, gathering and maintaining the data needed, and completing and reviewing the collection of information. Send comments regarding this burden estimate or any other aspect of this collection of information, including suggestions for reducing the burden, to Department of Defense, Washington Headquarters Services, Directorate for Information Operations and Reports (0704-0188), 1215 Jefferson Davis Highway, Suite 1204, Arlington, VA 22202-4302. Respondents should be aware that notwithstanding any other provision of law, no person shall be subject to any penalty for failing to comply with a collection of information if it does not display a currently valid OMB control number.</p> <p><b>PLEASE DO NOT RETURN YOUR FORM TO THE ABOVE ADDRESS.</b></p>					
<b>1. REPORT DATE (DD-MM-YYYY)</b> 21-07-2010		<b>2. REPORT TYPE</b> Final Report		<b>3. DATES COVERED (From – To)</b> 20 February 2009 - 20-Feb-10	
<b>4. TITLE AND SUBTITLE</b>  Surface-Chemical and -Morphological Influences on Adhesion and Friction: The Use of High-Throughput, Gradient Approaches			<b>5a. CONTRACT NUMBER</b> FA8655-09-C-4005		
			<b>5b. GRANT NUMBER</b>		
			<b>5c. PROGRAM ELEMENT NUMBER</b>		
<b>6. AUTHOR(S)</b>  Professor Nicholas D Spencer			<b>5d. PROJECT NUMBER</b>		
			<b>5d. TASK NUMBER</b>		
			<b>5e. WORK UNIT NUMBER</b>		
<b>7. PERFORMING ORGANIZATION NAME(S) AND ADDRESS(ES)</b> ETH Zurich Wolfgang-Pauli-Strasse 10 Zürich CH-8093 Switzerland				<b>8. PERFORMING ORGANIZATION REPORT NUMBER</b>  N/A	
<b>9. SPONSORING/MONITORING AGENCY NAME(S) AND ADDRESS(ES)</b>  EOARD Unit 4515 BOX 14 APO AE 09421				<b>10. SPONSOR/MONITOR'S ACRONYM(S)</b>	
				<b>11. SPONSOR/MONITOR'S REPORT NUMBER(S)</b> SPC 09-4005	
<b>12. DISTRIBUTION/AVAILABILITY STATEMENT</b>  Approved for public release; distribution is unlimited.					
<b>13. SUPPLEMENTARY NOTES</b>					
<b>14. ABSTRACT</b> <p>Pull-off curve measurements in both humidity-controlled air and under water will be carried out by means of AFM and Hysitron adhesion experiments. Tip geometry will be controlled through use of micron-scale glass beads or conospherical diamond tips. Maximum loads and loading rates will be selected to maintain an elastic response of the materials supporting the gradient films and textures. For the experiments with the Hysitron apparatus, we will follow protocols for quasi-static and dynamic adhesion measurements developed by Wahl and coworkers.</p> <p>Initial experiments would involve the simplest morphological gradients (monodisperse beads in a surface-concentration gradient), and would be followed by the more complex, sandblasted gradients. These gradients are of a kind that have already been fabricated many times in our laboratory and yet the experimental data obtainable with them would, to our knowledge, be absolutely unique and highly suitable for comparison with theory. Chemical gradients would be measured and results compared to the (mostly AFM) literature, prior to adding them to the morphological gradients to detect synergistic behavior. For gradient patterns on silicone elastomers, the elastomer properties can be selected to allow us to explore adhesion hysteresis due to gradient surface effects while the underlying mechanics can be expected to follow JKR behavior.</p> <p>Initial experiments would involve the microtribometer, since it is a relatively straightforward method to minimize surface damage and to obtain quantitative data. In tandem with this, AFM experiments would be carried out, followed by macroscopic measurements, when possible. Friction experiments (always as a function of both load and velocity, when possible) would be undertaken on systems for which the adhesion properties had already been characterized, and therefore morphology would be studied, then chemistry, and finally the combination.</p>					
<b>15. SUBJECT TERMS</b> EOARD, Friction and wear, surface materials, surface adhesion					
<b>16. SECURITY CLASSIFICATION OF:</b>			<b>17. LIMITATION OF ABSTRACT</b> UL	<b>18. NUMBER OF PAGES</b>  14	<b>19a. NAME OF RESPONSIBLE PERSON</b> WYNN SANDERS, Maj, USAF
<b>a. REPORT</b> UNCLAS	<b>b. ABSTRACT</b> UNCLAS	<b>c. THIS PAGE</b> UNCLAS			<b>19b. TELEPHONE NUMBER</b> <i>(Include area code)</i> +44 (0)1895 616 007

# Technical Progress Report

EOARD Grant 094005  
Award # FA8655-09-C-4005

## Surface-Chemical and -Morphological Influences on Adhesion and Friction: The Use of High-Throughput, Gradient Approaches

For the period: 02/20/09-02/20/10

### Principal Investigator

Nicholas Spencer  
Laboratory for Surface Science and Technology  
Department of Materials  
Swiss Federal Institute of Technology  
ETH Zurich, HCI H523, CH-8093 Zurich  
Switzerland

### Cognizant Program Manager

Maj. Wynn Sanders  
European Office of Aerospace  
Research and Development  
223/231 Old Marylebone Rd  
London NW1 5TH  
UK

### AFOSR Technical Contact

Maj. Michelle Ewy, PhD  
875 North Randolph St.  
Suite 325, Room 3112  
Arlington, VA 22203  
USA

## 1. Introduction

Friction and adhesion are fundamental properties of material interfaces that are as important to virtually every technology as they are familiar in everyday life. Despite the central roles of these interrelated material interface properties, our understanding of their fundamental nature remains surprisingly primitive. While tribology is normally taken to encompass science and technology relating to friction, lubrication, and wear, these phenomena are inextricably linked to adhesion. Friction, for example, has been described by Israelachvili as being equivalent to “adhesion hysteresis”<sup>1</sup>, and our own work has demonstrated this phenomenon on a nanoscopic level<sup>2</sup>. Adhesive wear, to give another example, is prevalent in systems as disparate as truck engines and hip implants.

Intuitively, we know that the surface chemistry influences tribological phenomena. Some surfaces are slippery, others are not, some surfaces are sticky, others are not. It is also evident in everyday life that surface morphology is important in determining friction and adhesion, but in a non-trivial way: sometimes roughness lowers friction, sometimes it increases it. In reality, adhesion is often the parameter that determines the relationship between morphology and friction. In the submicron world, adhesion dominates over all other forces. It thus becomes critical to understand adhesion and the way in which it depends on the nature of the surfaces involved. Such understanding will lead to procedures that can be used to modify adhesion, and hence friction, in a predictable manner.

In this feasibility project, emphasis was placed on the establishment of methodologies and the initial evaluation of the influence of surface morphology and chemistry on adhesion and friction. The key approach, in addition to those necessary for measuring the relevant surface forces, was the application of gradients of morphology and chemistry, which facilitates very rapid data acquisition and comparison with existing theories.

The **Approach** involved the use of gradients in surface morphology and chemistry for experiments involving adhesion and friction on the nano, micro, and macro scales. The significant advantage of gradients is that a single parameter (chemistry or morphology) or a pair of such parameters can be varied while *all other parameters are held constant*. This combinatorial approach significantly increases the reproducibility of the experiments in comparison to traditional methods, while allowing a vast parameter space to be explored very rapidly.<sup>1</sup>

The **Air Force Relevance** of the project is significant. Adhesion and friction issues abound in AF-relevant microtechnologies (microsatellites, MEMS, electrical contacts) as well as in many macrosystems (bearing systems, tire-runway contact, etc) that can be of equal ultimate importance to mission success.

---

1. J. N. Israelachvili, Y.-L. Chen, and H. Yoshizawa, *J. Adhesion Sci. Technol.* 1994, 8, 1231

2. A. Marti, G. Hähner, and N. D. Spencer, *Langmuir* 1995, 11, 4632-4635



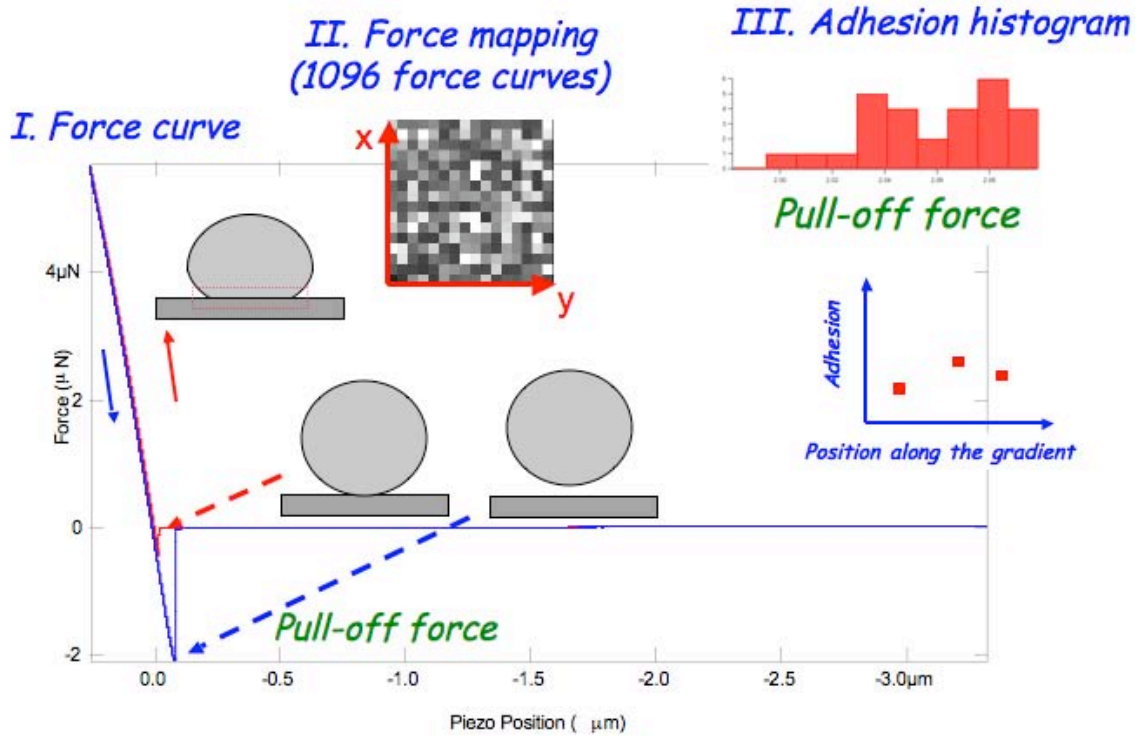


Figure 2. AFM adhesion data acquisition by means of force-mapping technique.

Atomic force microscopy force mapping (the acquisition of multiple force curves over a limited area) was used to gain sufficient statistics of adhesion forces, and force histograms were constructed from the resulting force measurements (Figure 2) at various positions along the morphology gradient.

### AFM Adhesion Measurements on a Gradient Surface in Air

A colloid-sphere (5  $\mu\text{m}$  in diameter, polyethylene) modified AFM tip was used to characterize the adhesion behavior on a 40 nm diameter particle gradient in air. Figure 3 shows the mean adhesion measured as a function of particle density. Different adhesion values were observed at locations where particle density is varied.

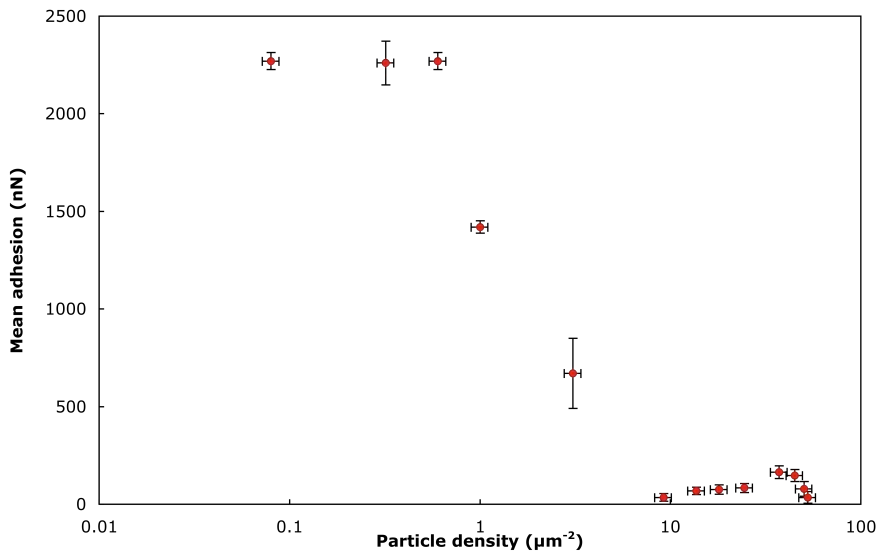


Figure 3. Adhesion between a polyethylene probe and a particle gradient in air.

### Simple JKR interpretation of data

By applying the Johnson, Kendall, and Roberts approach to interpreting the data, the results of the adhesion experiments can be readily rationalized as being due to single or multiple contacts on the underlying nanoparticle-covered surface, and the measured adhesion values seem reasonable for the assumed contact geometries in the low and high pull-off force regions (Figure 4).

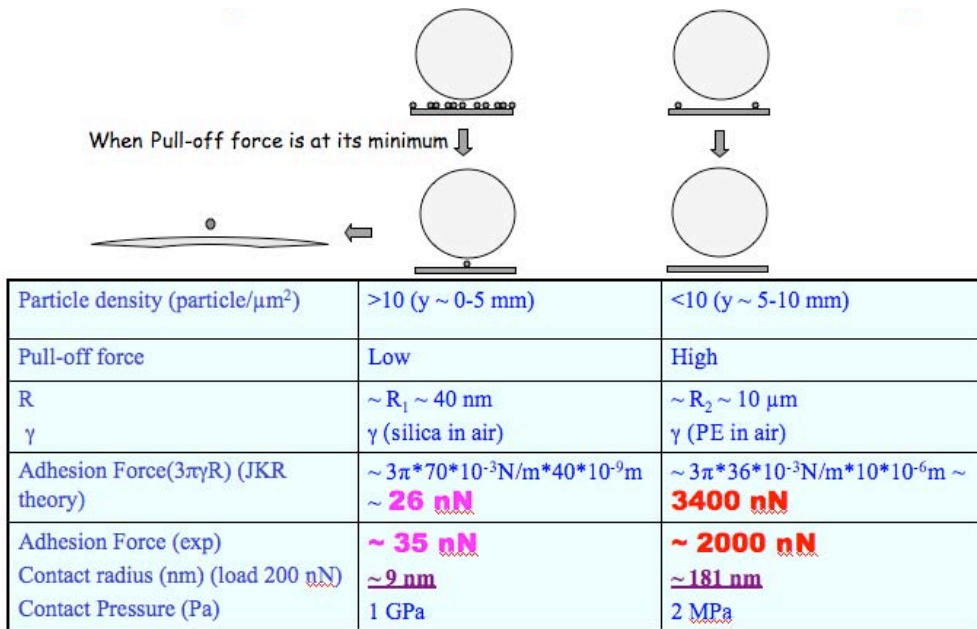


Figure 4. Simple JKR analysis of the contact situation, where either single particle or substrate contacts are considered.

### AFM Measurements of Friction on a Gradient Surface in Air

Friction measurements in air were made at various points along the nanoparticle gradient by means of AFM, while the load and velocity were varied. The results are summarized in Figure 5. While Amontons-like behavior was observed at the 0 mm position (high

particle coverage), no load dependence was observed at the end where no nanoparticles were present. This suggests that the latter situation was dominated by adhesion effects. While at high particle density no velocity dependence was observed, a marked velocity dependence was observed on the particle-free surface. Interestingly, in the middle of the gradient, a transitional behavior was observed, where Amontons-like behavior was apparent at low loads, and load-independent behavior at high loads. This also marked the point at which velocity dependence was only observable at higher loads.

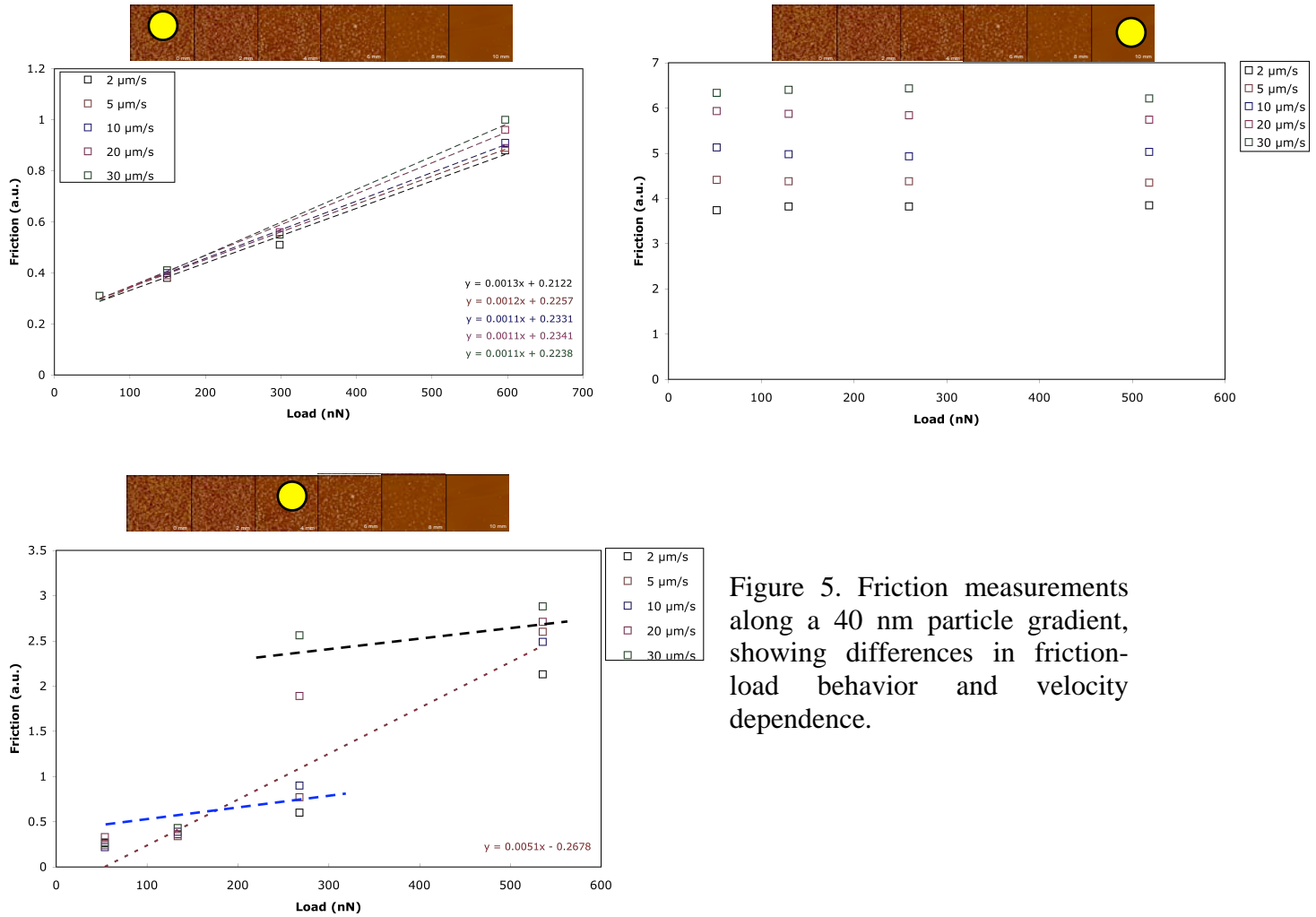


Figure 5. Friction measurements along a 40 nm particle gradient, showing differences in friction-load behavior and velocity dependence.

## Relating Friction to Adhesion in Air

Figure 6 plots the adhesion and friction together as a function of particle density. Similar trends can be observed and indicates the adhesion and friction are closely related in air.

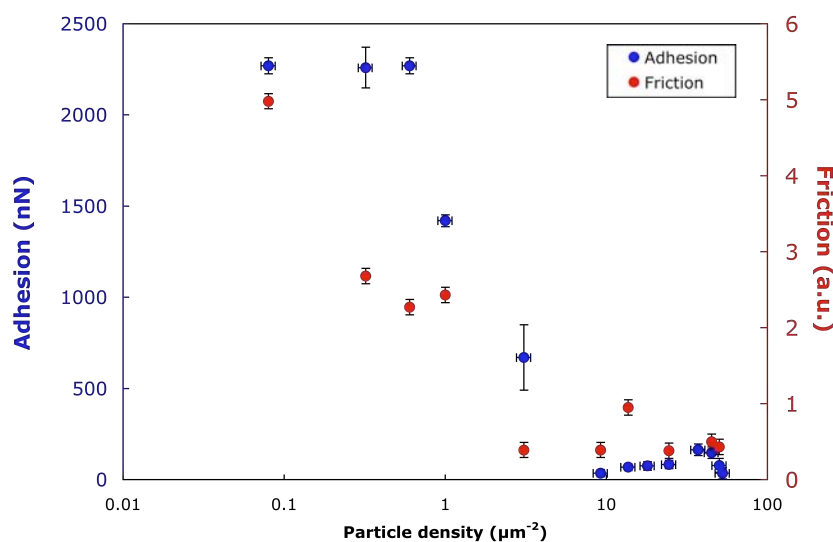


Figure 6. Mean adhesion and friction force between a polyethylene sphere and a 40 nm particle gradient in air as a function of nanoparticle density on the gradient substrate.

### Adhesion and Friction measurements in water

The dominating forces between a polyethylene sphere and a silica nanoparticle gradient in air are both van der Waals and capillary forces. Once the whole system is transfer to an aqueous environment, the situation is different. The van der Waals force is reduced, the capillary forces are now absent. The new dominating force is the electrical double layer forces due to the surface charge on both interfaces. It is shown in Figure 7, both adhesion and friction are reduced and they are independent of the nanoparticle density.

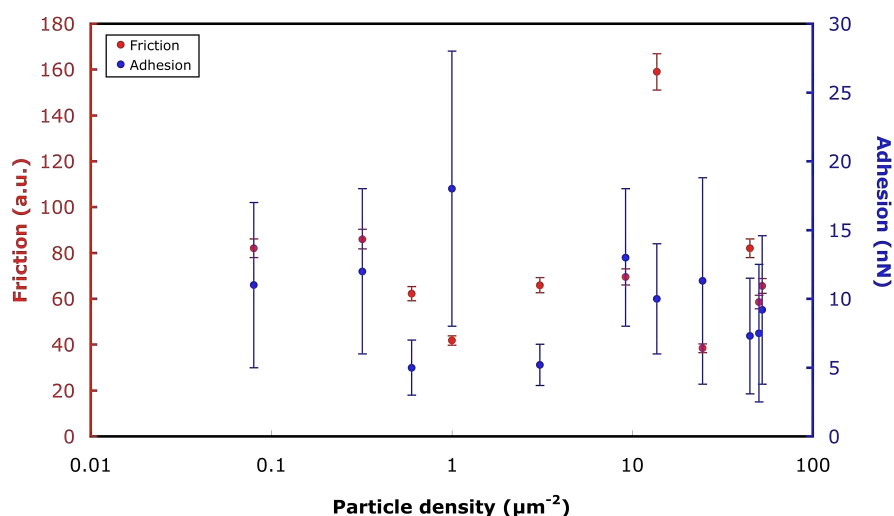


Figure 7. Adhesion and friction between a polyethylene sphere and a silica nanoparticle gradient in water.



### Adhesion measurements in perfluorodecalin (PFD)

To simplify the interactions between the polyethylene sphere and the silica nanoparticle gradient, we have employed a low-dielectric-constant medium – perfluorodecalin (PFD). In such a system, only van der Waals forces act between the PE sphere and the silica substrate. To improve the statistics, new nanoparticle gradients formed by 10 nm (in diameter) sized particles were successfully produced using the same method. Figure 8 shows the measured adhesion force between a PE sphere and a 10 nm silica nanoparticle gradient in perfluorodecalin as a function of the nanoparticle density on the substrate. On the smooth end of the gradient (i.e. the particle density is close to 0 particles per  $\mu\text{m}^2$ ), the measured adhesion is about 10 nN. For the rest of the gradient, adhesion is between 2 and 4 nN, regardless of the nanoparticle density.

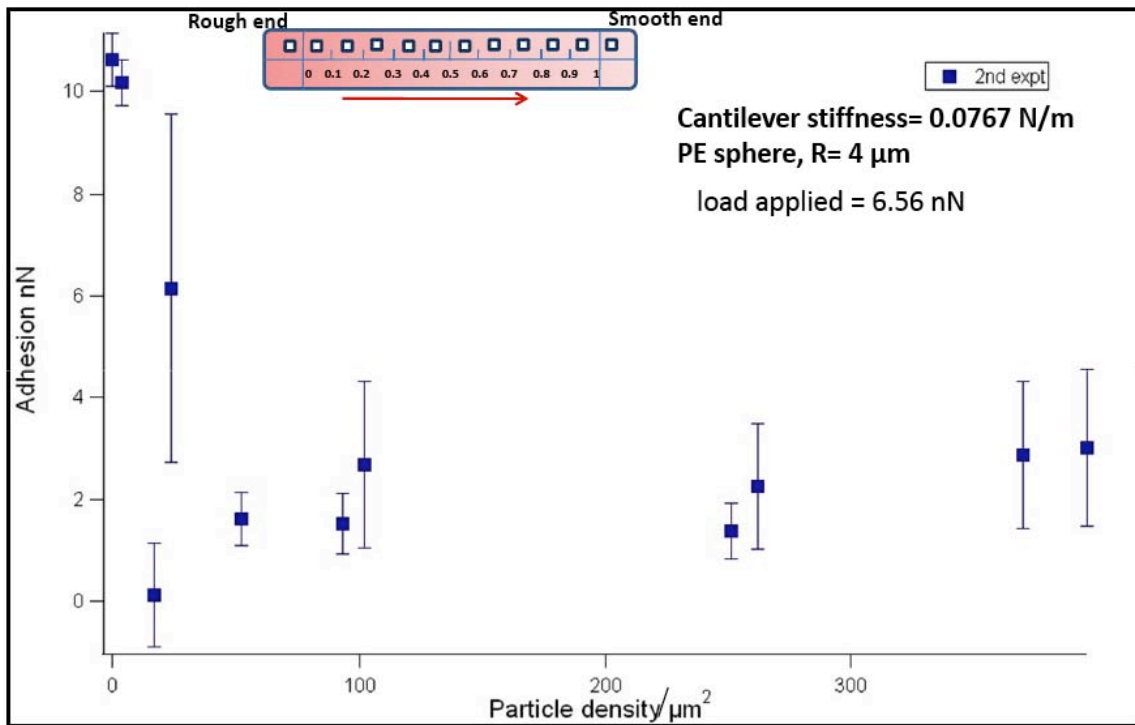


Figure 8. Adhesion between a PE sphere and a 10 nm nanoparticle gradient in perfluorodecalin.

### Friction measurements in perfluorodecalin (PFD)

Figure 9 shows the friction measured between a PE sphere and a 10 nm particle gradient in PFD. A slightly higher friction force was measured on the smooth end of the particle gradient. At all positions along the gradient substrate, the friction increases as a function of the normal force. However, there is little difference in the measured friction force on different parts of the substrate; that is, the friction force is independent of the particle density on the gradient.

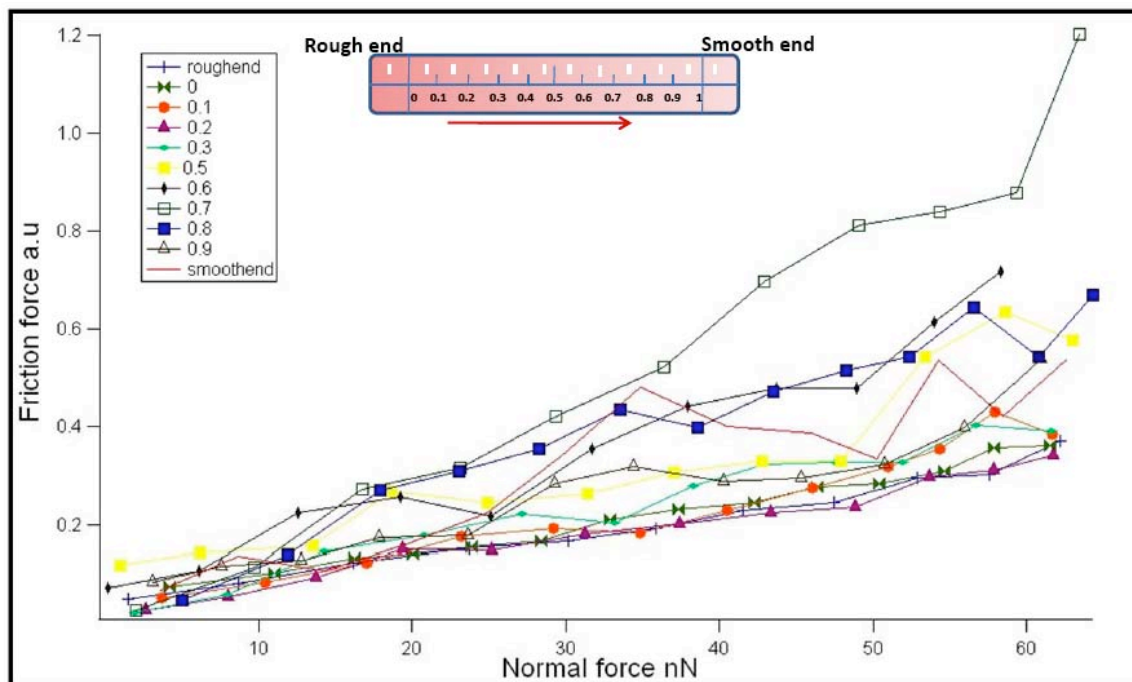


Figure 9. Friction between a PE sphere and a 10 nm nanoparticle gradient in perfluorodecalin as a function of normal load.

### Adhesion & Friction measurements in PFD with a larger PE sphere

The influence of the size of polyethylene sphere on adhesion was also studied. A PE sphere with a diameter of 26  $\mu\text{m}$  was used, in comparison to earlier experiments in which an 8  $\mu\text{m}$ -diameter sphere was used. Figure 10 shows the adhesion measured between the PE sphere and the particle gradient in PFD. When the particle density is less than 20 particles per  $\mu\text{m}^2$ , an increase in adhesion with decreasing particle density was seen and the highest adhesion was observed on the smooth end of the gradient. This value is around 11 nN, which is comparable to the previous experiment when a smaller PE sphere was used. When the particle density is greater than 20 particles per  $\mu\text{m}^2$ , the adhesion is around 2 nN and is independent of particle density. Such results agree with the previous experiment when a smaller PE sphere was used, but the statistics are improved by virtue of the larger contact area.

The friction measured between the larger polyethylene sphere and silica nanoparticle gradient is shown in Figure 11. Once again, the friction is seen to increase with increasing normal load regardless of the nanoparticle density. For normal loads less than about 60 nN, the friction increases linearly with increasing load. At higher loads, the friction continues to increase but no longer follows Amontons' law.

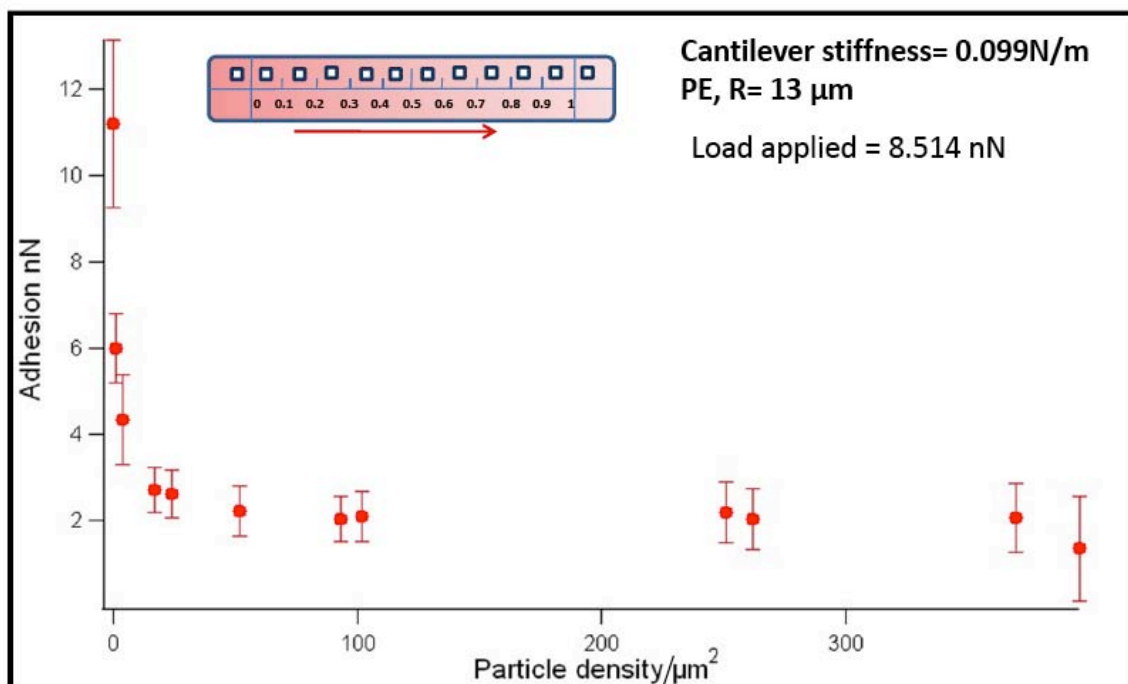


Figure 10. Adhesion between a 26  $\mu\text{m}$  (in diameter) polyethylene sphere and a 10 nm (in diameter) nanoparticle gradient in PFD.

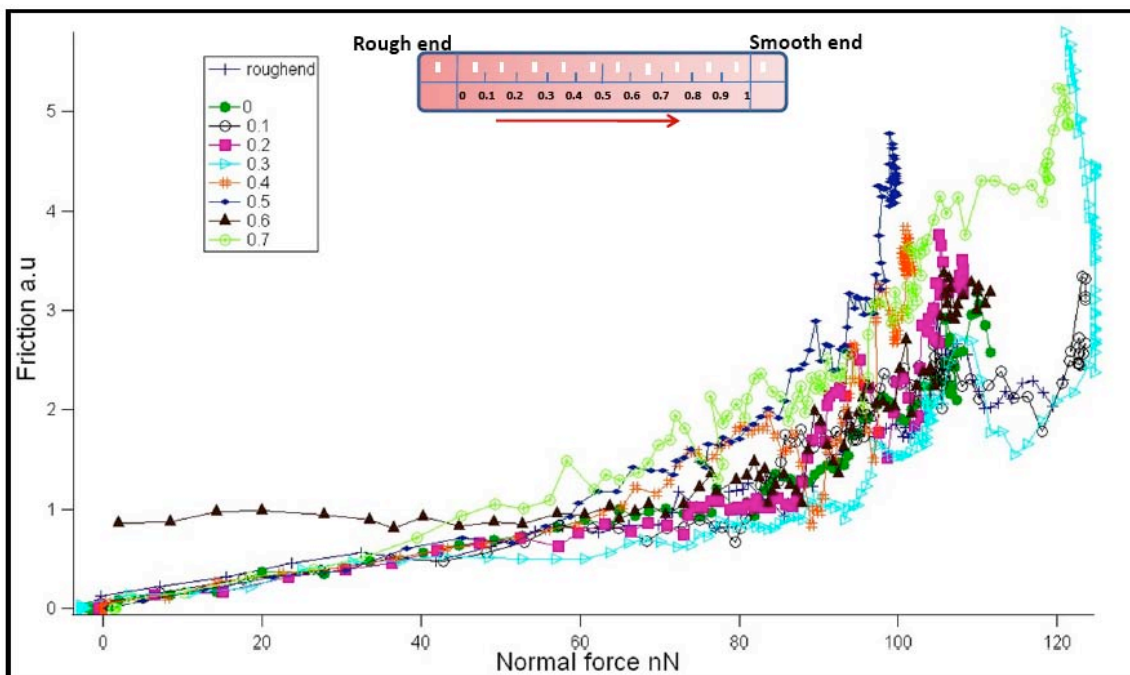


Figure 11. Friction between a 26  $\mu\text{m}$  (in diameter) polyethylene sphere and a 10 nm (in diameter) nanoparticle gradient in PFD.

## Adhesion & Friction measurements in PFD with a higher load

The adhesion and friction were also measured at a higher range of loads by employing a stiffer AFM cantilever. In these experiments, a cantilever with a spring constant of 5.48 N/m was used, more than 50 times stiffer than those previously used ( $< 0.1$  N/m). The adhesion as a function of particle density (Figure 12) follows the same trend as for the earlier experiments, but with higher adhesion forces. Figure 13 shows the friction-vs-load plot in the regime of higher loads. Over this range of loads, Amontons' law is followed, the friction increasing in direct proportionality with normal load up to the highest loads tested. In these experiments, however, there does not appear to be any clear dependence of the friction on the density of nanoparticles on the gradient surface.

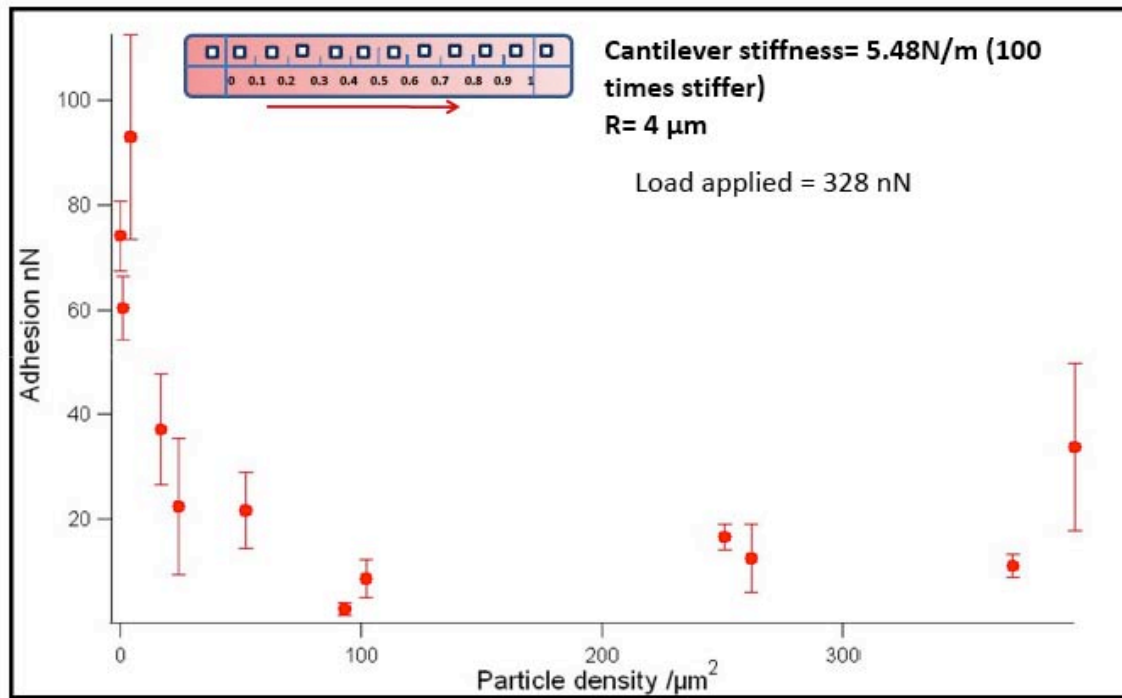


Figure 12. Adhesion between a PE sphere and a 10 nm nanoparticle gradient in perfluorodecalin, measured at a higher range of loads using a stiff cantilever.

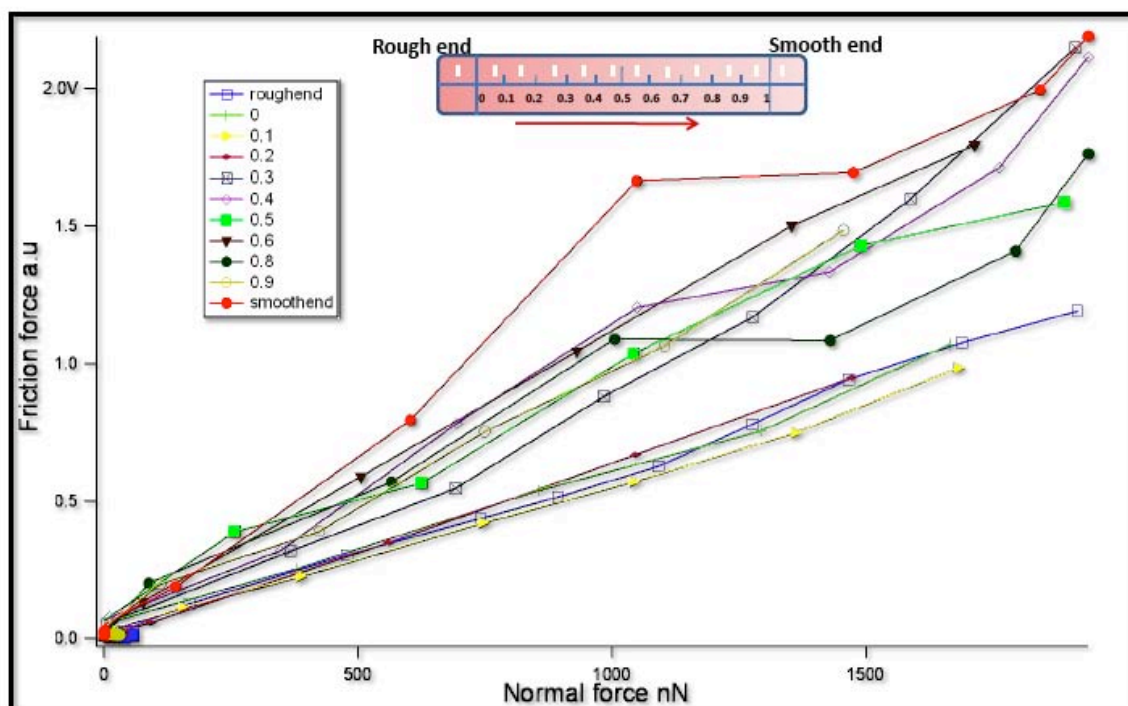


Figure 13. Friction between a PE sphere and a 10 nm nanoparticle gradient in perfluorodecalin, measured at a higher range of loads using a stiff cantilever.

#### 4. Summary of the results

	Air		Water		PFD	
Particle density	High	Low	High	Low	High	Low
Adhesion	Low	High	Small adhesion, no dependence on particle density		Small adhesion, no dependence on particle density	Slightly higher adhesion
Friction	Low	High	No dependence on particle density		No dependence on particle density	Slightly higher friction

Figure 14. Summary of adhesion and friction between a polyethylene (PE) sphere and a silica nanoparticle gradient in air, water and perfluorodecalin (PFD).

The correlation between adhesion and friction was most clearly seen in air, where the adhesion varies from the order of 100 nN to 2000 nN along the particle density gradient. It was also shown in air that the friction is either load-dependent or velocity-dependent, influenced by the nanoparticle density on the substrate. In water, the adhesion is reduced to 5 - 10 nN and neither adhesion nor friction show any dependence on the nanoparticle density on the substrate. In PFD, the adhesion is higher (10 nN) when there are no nanoparticles on the substrate. For the rest of the gradient, both adhesion and friction

show no dependence on the particle density.

In PFD, we have also studied the influence of the size of the PE sphere and better quality adhesion data was obtained when a larger PE sphere was used (26  $\mu\text{m}$ -diameter). At higher loads, adhesion increases and follows the same trend as at the lower load regime. Friction behavior follows Amontons' law and depends linearly on the applied load.

## ***5. Outlook***

Friction measurements reported above have been in arbitrary units, and efforts to calibrate our lateral force measurement setup are currently in progress. These will be implemented in the successor project.

While a simple JKR approach has been taken to interpret the data so far, it is hoped that further experiments will provide a basis for the testing of alternative theories.

Once the current series of morphological gradient experiments is complete, the introduction of surface-chemical variables on the adhesion and friction measurements can be contemplated.

## ***6. Personnel***

Postdoc: Dr Lucy Clasohm, ETH Zurich

PhD Student: Shivaprakash Ramakrishna, ETH Zurich

Consultant: Dr Kathy Wahl, Naval Research Lab, Washington, DC